One-Shot Localization with Random Wavefronts

Burak Bilgin[1], Jy-Chin Liao[1], Hou-Tong Chen[2], Chun-Chieh Chang[2], Sadhvikas Addamane[3], Michael P. Lilly[3], Daniel M. Mittleman[4], Edward W. Knightly[1]
[1] Rice University, Houston, TX, USA
[2] Los Alamos National Laboratory, Los Alamos, NM, USA
[3] Sandia National Laboratories, Albuquerque, NM, USA
[4] Brown University, Providence, RI, USA

ABSTRACT

The next generation of wireless networks will utilize highly directional beams to overcome the path loss at high frequencies, requiring angle inference during link establishment. Furthermore, the integration of location-based services into the wireless infrastructure is rapidly increasing, bringing in a significant demand for an integrated fast localization scheme. In this work, we present a first-of-its-kind one-shot angular localization method that is carried out with a reconfigurable architecture that unlocks ISAC functionality. Specifically, we use an electrically tunable metasurface with broadband response to generate wavefronts that are randomized across the angular space with diverse wideband amplitude and phase observations, corresponding to a collection of angle-unique one-shot beacons. Our results show down to 0.26° mean absolute error at 20 dB SNR, an order of magnitude improvement over the recently proposed one-shot solutions based on leaky-wave antennas (LWAs), in addition to having wider area coverage and less stringent bandwidth requirements.

CCS CONCEPTS

• **Networks** → **Location based services**; • **Hardware** → **Wireless devices**.

KEYWORDS

mmWave/sub-THz, reconfigurable metasurfaces, one-shot localization, link establishment

Publication rights licensed to ACM. ACM acknowledges that this contribution was authored or co-authored by an employee, contractor or affiliate of the United States government. As such, the Government retains a nonexclusive, royalty-free right to publish or reproduce this article, or to allow others to do so, for Government purposes only.

ACM MobiCom '24, November 18–22, 2024, Washington D.C., DC, USA

© 2024 Copyright held by the owner/author(s). Publication rights licensed to ACM.

ACM ISBN 979-8-4007-0489-5/24/11…$15.00
https://doi.org/10.1145/3636534.3698225

ACM Reference Format:
Burak Bilgin[1], Jy-Chin Liao[1], Hou-Tong Chen[2], Chun-Chieh Chang[2], Sadhvikas Addamane[3], Michael P. Lilly[3], Daniel M. Mittleman[4], Edward W. Knightly[1]. 2024. One-Shot Localization with Random Wavefronts. In *The 30th Annual International Conference on Mobile Computing and Networking (ACM MobiCom '24), November 18–22, 2024, Washington D.C., DC, USA.* ACM, New York, NY, USA, 6 pages. https://doi.org/10.1145/3636534.3698225

1 INTRODUCTION

Angular localization of wireless nodes is a fundamental capability for future integrated sensing and communication (ISAC) systems [1, 2]. As the implementation of location-based services over wireless networks becomes increasingly ubiquitous towards 6G and wavefront engineering emerges as an integral part of establishing wireless links in mmWave and sub-THz bands [3, 4], low-latency localization becomes essential to offer such functionalities while avoiding outages due to mobility. Recently, "one-shot" location discovery became a pivotal component to realizing low-latency angular localization [5–12]. However, the architectures proposed in these works for one-shot localization are static, i.e., the transmission characteristics are not reconfigurable after fabrication, thus resulting in a significant setback in realizing efficient ISAC systems, where the ability to engineer the transmitted wavefronts for both communication and sensing dynamically is essential.

In this work, we present a first-of-its-kind one-shot angular localization method with a reconfigurable architecture that offers dynamic amplitude and phase modulation over a wide band, and we report an order of magnitude improvement in estimation error compared to leaky-wave antennas (LWAs). To realize our method, we generate sub-THz beacon signals that are unique to each angle of departure by randomizing the transmitted wavefront's amplitude and phase distribution over the transmitter's field of view (FoV). We use a broadband sub-THz metasurface that consists of sub-wavelength-scale resonators with continuously tunable and frequency-diverse amplitude and phase responses through column-wise separated analog voltage biasing. Moreover,

our reconfigurable architecture enables the realization of effective communication tools through the same transmitting aperture and thus is a crucial component in realizing efficient ISAC systems in 6G networks.

The prior work related to our method can be categorized into two fields:

One-Shot Localization. Several works demonstrated one-shot location discovery methods leveraging the dispersive angle-frequency relation of a THz leaky-wave antenna (LWA) [5–9]. However, LWAs are limited to an effective angle estimation field of view (FoV) of $\sim 70^\circ$, with average estimation error reported between $1^\circ - 3^\circ$, both due to their smooth convex angle-frequency function. Furthermore, the transmission characteristics of LWAs are static, i.e., they are limited to the same dispersive gain pattern for communication. Similarly, frequency-diverse methods based on lens-integrated cavities [10, 11] or non-reconfigurable metasurfaces [12] all use static hardware, rendering reconfiguration for effective communication tools impossible. In contrast, with our approach, we not only offer one-shot localization with finer resolution, wider FoV, and efficient bandwidth usage compared to LWAs but also unlock ISAC functionality through our reconfigurable architecture.

Reconfigurable Methods. While various methods using reconfigurable metasurfaces have been developed to improve latency and accuracy compared to Transmit Sector Sweep (TXSS) [13, 14], including the use of random narrowband angular signatures [15–18] based on compressive sensing framework [19–21], or harmonic frequency signatures generated by periodic-time modulation [22–27], they cannot be realized in one-shot. In contrast, our work realizes one-shot localization, a sensing paradigm critical to unlocking the data rates envisioned in 6G networks, with a reconfigurable architecture through carefully designing wideband beacons.

2 PROBLEM FORMULATION

In this section, we present the problem scenario and describe how our solution achieves one-shot fine-resolution angular localization through its key design features.

In one-shot localization, the ultimate goal is to design a set of wideband beacon signals that have unique amplitude and phase distributions at any given angle within the FoV of the transmitter:

$$h(\theta_k) = [h(f_1, \theta_k)\ h(f_2, \theta_k)\ \ldots\ h(f_L, \theta_k)]^T\ \forall \theta_k \in \Theta \qquad (1)$$

where $\Theta = \{\theta_1, \theta_2, \ldots, \theta_K\}$ is the discretized FoV and $B = \{f_1, f_2, \ldots, f_L\}$ is the beacon bandwidth with L channels. A visual representation of the beacon transmission in our architecture is shown in Figure 1.

Subsequently, a receiver collecting a noisy beacon signal $\overline{h} = h + \mathcal{N}(0, \sigma^2)$ can perform angle of departure estimation θ^* according to the pre-characterized beacon $h(\theta)$ closest in Euclidean distance to $\overline{h}$:

$$\theta^* = \arg\min_{\theta \in \Theta} \|\overline{h} - h(\theta)\|_2^2 \qquad (2)$$

In our work, we propose to dynamically generate sub-THz beacons that are randomized in amplitude and phase across the FoV to maximize inter-beacon distance. In contrast to a smooth and convex angle-frequency function, a randomized pattern minimizes the similarity of beacons corresponding to adjacent angles. Furthermore, we generate said beacon signals with reconfigurable hardware, providing ISAC functionality essential for 6G networks. We incorporate two key design features in our method:

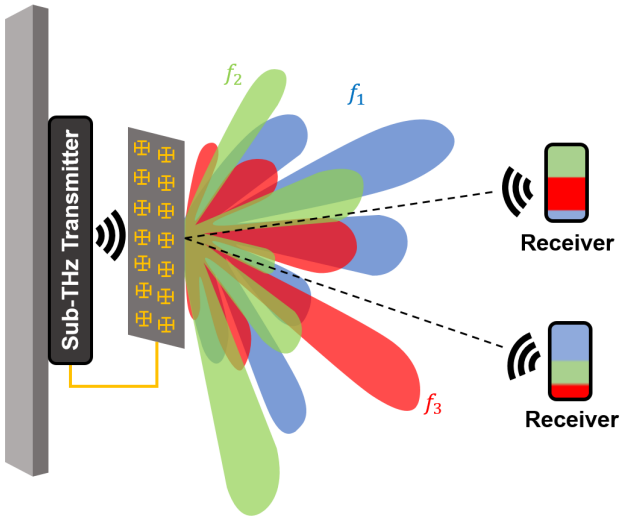

Figure 1: Proposed one-shot localization system.

1- Metasurface with Continuously Tunable EM Response. We design a transmissive and electrically tunable metasurface with a strong resonance response in the sub-THz band, envisioned to be a critical network component in 6G networks. Unlike the binary phase response of the PIN-diode elements typically used in the mmWave region, our subwavelength-scale split-ring resonators have continuously tunable amplitude and phase response, both unlocking a wider response domain over which to generate randomized beacons and allowing fine-resolution amplitude and phase modulation necessary for sub-THz communication.

2- Wideband Wavefront Randomization through Frequency-Diverse Response. Through carefully designing the geometry of our resonators, we realize a frequency-diverse inductive-capacitive (LC) resonance in the 125-155 GHz band [28]. Furthermore, combining this with a set of bias voltage configurations that uniformly randomize the

complex E-field response at each metasurface "pixel", we generate unique beam patterns at each frequency component over the band.

3 METASURFACE AND BEACON DESIGN

In this section, we describe the metasurface design and fabrication process as well as the voltage configuration design.

To generate our wideband angle-unique beacons, we use the metasurface shown in Figure 2a. The 2.5 cm x 2 cm metasurface is fabricated on a THz-transmissive 2 μm-thick n-doped GaAs layer grown on a semi-insulating GaAs wafer [29]. The cross-shaped split-ring gold resonators are layered on the semiconductor substrate through photolithography. The combination of the split-ring resonators with the semiconductor substrate yields a Schottky junction, where the carrier density of the substrate at the corners of each resonator can be tuned by reverse biasing the resonators, enabling continuous and dynamic tuning of the amplitude and phase response of the resonator to incident sub-THz EM waves [28, 30]. The same bias voltage is fed to each "pixel," consisting of 6x155 columns of resonators, with a total of 16 pixels. The resonators are fabricated with an edge length of 163 μm, line width of 6 μm, and gap width of 2 μm, corresponding to an LC-resonance response at 145 GHz. The metasurface's amplitude and phase response tunable range are shown in Figures 2c and 2d, where all pixels are fed with a uniform bias voltage. In addition to the resonance observed at 145 GHz, the metasurface is capable of frequency-diverse amplitude and phase modulation over the 127-152 GHz band.

3.1 Beacon Design

To design wideband angle-unique beacons, we first mathematically characterize the signal modulation capabilities of our metasurface. As visualized in Figure 1, a metasurface illuminated by a sub-THz transmitter generates a wideband signal. At azimuth angle θ, each frequency component $h_r(f,\theta)$ observed by a receiver can be characterized as a sum of the waves emitted by the 16 metasurface pixels, with each pixel modulating the wave according to its frequency response and applied bias voltage:

$$h_r(f,\theta) = \sum_{p=1}^{P} \frac{1}{r_p} e^{i\frac{2\pi f}{c} r_p} A_p(f,V) e^{i\phi_p(f,V)} A_{in} e^{i2\pi f t} \quad (3)$$

where $r = \{r_1, r_2, \cdots, r_P\}$ is the set of distances from each pixel to the receiver, $A_{in}e^{i2\pi ft}$ is the transmitter signal, and $A_p exp(i\phi_p)$ is the complex E-field response of the p^{th} pixel. We omit the elevation angle for ease of analysis.

In our work, we design each pixel's complex field response $A_p exp(i\phi_p)$ to be an independent and identically distributed (i.i.d.) uniform random variable, defined within the metasurface's modulation range at the resonance frequency of 145 GHz. Combined with the varying pixel-to-receiver distances r, the sum of the resulting random modulations corresponds to a unique amplitude and phase value observed at each $\theta \in \Theta$ at this frequency. To realize this set of randomly selected pixel responses, we then determine the corresponding control voltages for each pixel $\mathcal{V} = \{V_1, V_2, ..., V_P\}$ through the precharacterized voltage-to-response function shown in Figure 2b. We refer to any given set of control voltages determined this way as a metasurface *configuration*.

Furthermore, by applying a metasurface configuration designed in the above manner, we uniquely randomize the pixels' responses also at neighboring frequencies, i.e., over the 125-155 GHz band. This is achieved through the spectrally diverse nature of the response function as seen in Figures 2c and 2d, in which a given bias voltage results in different amplitude and phase responses at different frequencies, and each pixel-receiver distance $r_i \in \{r_1, r_2, \cdots, r_P\}$ corresponding to a wavelength-dependent propagation phase at the receiver angle θ, resulting in a unique complex superposition of the randomly modulated signals at each frequency. Ultimately, our reconfigurable architecture can generate random wavefronts across a wide band. For one-shot localization, we assign the complex field values across the discrete FoV $\Theta = \{\theta_1, \theta_2, ..., \theta_K\}$ over the bandwidth $B = \{f_1, f_1, ..., f_L\}$ in a beacon-angle map H_{LK}.

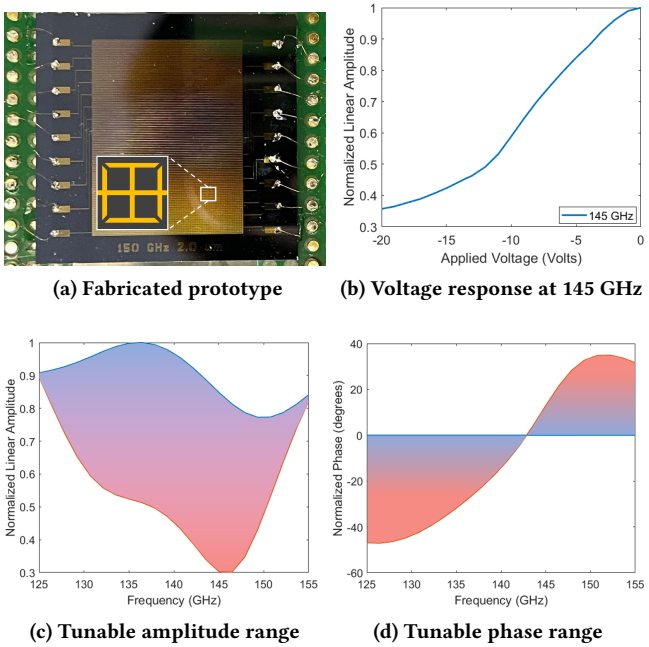

(a) Fabricated prototype (b) Voltage response at 145 GHz

(c) Tunable amplitude range (d) Tunable phase range

Figure 2: Metasurface design and response.

4 OVER-THE-AIR EXPERIMENTS

In this section, we present an experimental characterization of our designed wavefronts as beacon signals for one-shot localization and analyze the angle estimation performance of our method.

4.1 Beacon Generation

Here, we experimentally generate wavefronts with the established design process and characterize them at different frequencies. As described in Section 3, each wavefront at a distinct frequency ideally exhibits a unique angular pattern due to the frequency-diverse metasurface response and wavelength-dependency of the superposed waves from each pixel. Consequently, a receiver listening over the bandwidth B is ideally able to identify the angle of departure of the signal thanks to the unique set of wavefronts corresponding to a unique set of received beacons at each angle.

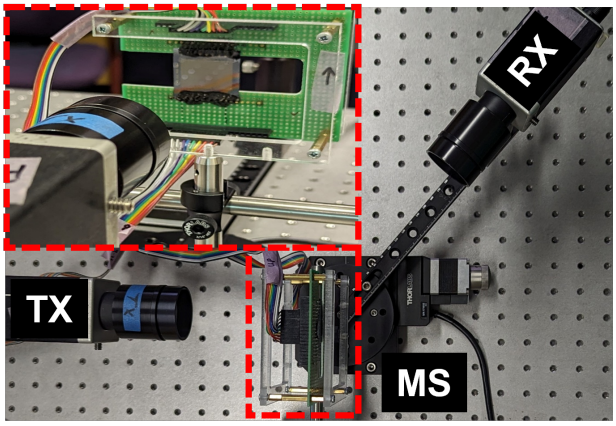

Figure 3: Experiment setup.

Experimental Setup. Our experimental setup is shown in Figure 3. We use a LUNA T-Ray 5000 Time-Domain Terahertz Spectroscopy (TDS) system, which provides sufficient bandwidth to characterize the generated wavefronts. In the setup, a transmitter sending broadband THz pulses illuminates the metasurface positioned 11 cm from its aperture, and a broadband directional receiver collects the generated signal over the FoV $[-50°, 50°]$ with a 0.1° step size at a fixed distance of 15 cm from the metasurface. The received signal is averaged 100 times at each angular location to ensure accurate beacon characterization. Similarly, the distance values are determined to characterize the randomness of the generated waves without the effect of experimental noise caused by the extremely low-power nature of the TDS system. We bias the functioning 7 pixels of the metasurface (pixels 1, 2, 4, 5, 6, 7, 8) using a National Instruments DAC card (NI PCIe-6738) with a configuration designed in the manner described in Section 3.

Results. We present in Figure 4 the amplitude and phase patterns generated by the designed configuration at frequencies 127.1, 140, and 151.4 GHz. Here, the x-axis shows the angles in the FoV, and the y-axis shows the amplitude and phase values in the top and bottom plots, respectively. The amplitude values are on a linear scale and normalized with respect to the highest observed value. We observe that the wavefront at each frequency exhibits a randomly distributed amplitude and phase pattern, and the distributions are unique across all frequencies. While each wavefront contains a main lobe with high amplitude near 0°, these main lobes differ in beamwidth and peak amplitude. Ultimately, the patterns show that the beacons generated over the 125-155 GHz band carry unique sets of amplitude and phase values corresponding to each angle of departure, verifying our architecture's wideband beacon generation capability.

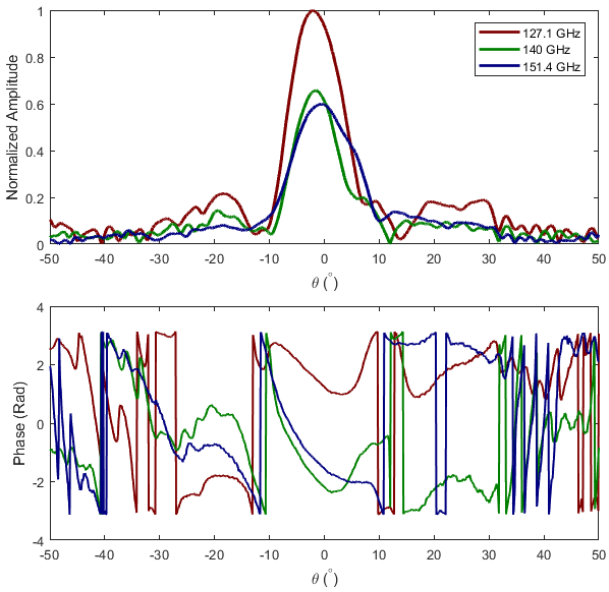

Figure 4: Randomized wideband E-field.

Findings. We conclude that the designed metasurface configuration successfully generated randomized amplitude and phase distributions at a fixed distance, and thus, the combination of such distributions over the metasurface's resonance band yields angle-specific wideband beacons. The high amplitude values observed in the broadside region are likely caused by the limited modulation efficiency of the current prototype, resulting in a fraction of the source signal passing through the metasurface unmodulated. Nonetheless, the wavefronts still exhibit diversity in beam shape, intensity, and phase in this region as a result of the modulated fraction. As such, the wavefronts generated in this experiment are collected into the beacon-angle map H_{LK} for the experimental

performance analysis of our one-shot localization scheme, as presented in the next section.

4.2 One-Shot Angle Estimation

In this experiment, we utilize the beacons generated in the previous section as a pre-characterized mapping to realize one-shot localization. Specifically, when a receiver in the FoV of the transmitter receives a beacon, it estimates the angle of departure as the minimizer of the function in Equation (2) by comparing the received beacon to each column of H_{LK}. Ideally, the wireless nodes in a typical ISAC system aim to perform communication and sensing with minimal bandwidth to avoid interference and prevent congestion. In our method, this goal corresponds to minimizing the number of rows of H_{LK} since the beacons are defined over a bandwidth B. Therefore, in this experiment, we investigate the change in angle estimation error achieved with our method over varying bandwidth values utilized in constructing H_{LK}.

Experimental Setup. We use the testbed introduced in Section 4.1 and repeat the data collection in the same manner, then add white Gaussian noise with 20 dB signal-to-noise ratio (SNR) to generate a set of test signals. Then, we perform angle estimation on each signal through a least squared error comparison between the received signal and the columns of the codebook and calculate the mean absolute error (MAE). Finally, we repeat the estimation 100 times with different noise values and calculate the maximum, minimum, and mean of MAE. Note that the data collection is performed over a discrete FoV with 0.1° resolution; thus, angle estimations in the correct angle "bin" equal zero error.

Results. Figure 5 shows the mean absolute error (MAE) calculated at 20 dB SNR in log-scale. The x-axis shows the varying bandwidth values used to construct the codebook with a 1.4 GHz step size, i.e., the frequency resolution of our system. The error bars show the range of MAE calculated across 100 trials. We observe a rapid improvement in average error with increasing bandwidth usage. In particular, when there are only two distinct frequencies used to construct the codebook, the observed MAE is 30.7°, which decreases to 0.26° with 18 components used in the 127-152 GHz band, demonstrating fine-resolution one-shot angle estimation.

Findings. Our results show that each additional frequency, i.e., row, in the set of pre-characterized beacons drastically improves estimation error due to the diverse wavefronts generated at each frequency. Furthermore, the observed 0.26° average error with 25 GHz bandwidth shows that statistical randomness in frequency response enables significantly more efficient bandwidth usage compared to non-random methods, e.g., the frequency dispersive function of LWAs, which requires more than 100 GHz bandwidth even with an optimized design [8]. As such, our method proves to be a critical facilitator for future ISAC systems where bandwidth is a limited resource.

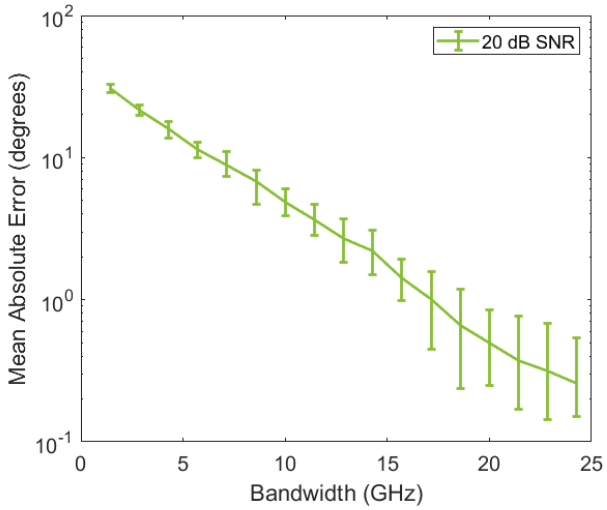

Figure 5: One-shot localization error performance.

5 CONCLUSION

In this work, we report a one-shot angular localization method with a reconfigurable architecture that enables communication and sensing functions to take place over the same aperture through its electrically tunable and frequency-diverse resonators. We experimentally demonstrate one-shot localization using spectrally and spatially randomized wavefronts and achieve an order of magnitude improvement in estimation error compared to LWA-based methods, in addition to improved field-of-view (100° vs 70°) and significantly more efficient bandwidth usage (25 GHz vs up to several hundred GHz). In future work, we envision further improving our method by carefully optimizing our design with respect to the frequency-unique characteristics of the metasurface and designing the accompanying network protocol that governs channel access and data transmission following localization. Furthermore, we aim to increase the transmission efficiency of our fabrication to further increase beacon diversity for small angles ([-10°, 10°]).

6 ACKNOWLEDGMENTS

BB, JL, and EK's research was supported by Cisco and Intel, by NSF grants 2402783, 2211618, 2148132, and 1955075, and by ARO DURIP grant W911NF-23-1-0340. DM's research was supported by NSF grants 2402781, 2211616, and 1954780. This work was performed, in part, at the Center for Integrated Nanotechnologies, an Office of Science User Facility operated for the U.S. Department of Energy (DOE) Office of Science by Los Alamos National Laboratory (Contract 89233218CNA000001) and Sandia National Laboratories (Contract DE-NA-0003525).

REFERENCES

[1] Zhiqiang Xiao and Yong Zeng. An overview on integrated localization and communication towards 6g. *Science China Information Sciences*, 65(3), 12 2021.

[2] Hui Chen, Hadi Sarieddeen, Tarig Ballal, Henk Wymeersch, Mohamed-Slim Alouini, and Tareq Y. Al-Naffouri. A tutorial on terahertz-band localization for 6g communication systems. *IEEE Communications Surveys & Tutorials*, 24(3):1780–1815, 2022.

[3] Innem V.A.K. Reddy, Duschia Bodet, Arjun Singh, Vitaly Petrov, Carlo Liberale, and Josep M. Jornet. Ultrabroadband terahertz-band communications with self-healing bessel beams. *Communications Engineering*, 2(1), 10 2023.

[4] Burak Bilgin and Edward W. Knightly. Metashield: a multi-function apsurrounding metasurface. In *Proceedings of the 17th ACM Workshop on Wireless Network Testbeds, Experimental Evaluation & Characterization*, WiNTECH '23, page 1–8, New York, NY, USA, 2023. Association for Computing Machinery.

[5] Yasaman Ghasempour, Rabi Shrestha, Aaron Charous, Edward Knightly, and Daniel M. Mittleman. Single-shot link discovery for terahertz wireless networks. *Nature Communications*, 11(1), 4 2020.

[6] Atsutse Kludze, Rabi Shrestha, Chowdhury Miftah, Edward Knightly, Daniel Mittleman, and Yasaman Ghasempour. Quasi-optical 3d localization using asymmetric signatures above 100 ghz. In *Proceedings of the 28th Annual International Conference on Mobile Computing And Networking*, MobiCom '22, page 120–132, New York, NY, USA, 2022. Association for Computing Machinery.

[7] Yasith Amarasinghe, Rajind Mendis, and Daniel M. Mittleman. Real-time object tracking using a leaky thz waveguide. *Opt. Express*, 28(12):17997–18005, Jun 2020.

[8] Hooman Saeidi, Suresh Venkatesh, Xuyang Lu, and Kaushik Sengupta. Thz prism: One-shot simultaneous localization of multiple wireless nodes with leaky-wave thz antennas and transceivers in cmos. *IEEE Journal of Solid-State Circuits*, 56(12):3840–3854, 2021.

[9] Harrison Lees, Daniel Headland, Shuichi Murakami, Masayuki Fujita, and Withawat Withayachumnankul. Terahertz radar with all-dielectric leaky-wave antenna. *APL Photonics*, 9(3), 2024.

[10] Mingxiang Stephen Li, Mariam Abdullah, Jiayuan He, Ke Wang, Christophe Fumeaux, and Withawat Withayachumnankul. Frequency-diverse antenna with convolutional neural networks for direction-of-arrival estimation in terahertz communications. *IEEE Transactions on Terahertz Science and Technology*, 14(3):354–363, 2024.

[11] Muhammad Ali Babar Abbasi, VF Fusco, Okan Yurduseven, and Thomas Fromenteze. Frequency-diverse multimode millimetre-wave constant-ϵ_r lens-loaded cavity. *Scientific Reports*, 10(1):22145, 2020.

[12] Tianyi Zhou, Huan Li, Dexin Ye, Jiangtao Huangfu, Shan Qiao, Yongzhi Sun, Weiqiang Zhu, Changzhi Li, and Lixin Ran. Short-range wireless localization based on meta-aperture assisted compressed sensing. *IEEE Transactions on Microwave Theory and Techniques*, 65(7):2516–2524, 2017.

[13] IEEE. Ieee 802.11az approved draft standard for information technology – amendment 4: Enhancements for positioning. *IEEE P802.11az/D7.0*, page 1–291, 2022.

[14] Pablo Picazo-Martinez, Carlos Barroso-Fernandez, Jorge Martin-Perez, Milan Groshev, and Antonio de la Oliva. Ieee 802.11az indoor positioning with mmwave. *IEEE Communications Magazine*, pages 1–7, 2023.

[15] Mingtuan Lin, Ming Xu, Xiang Wan, Hanbing Liu, Zhaofeng Wu, Jibin Liu, Bowen Deng, Dongfang Guan, and Song Zha. Single sensor to estimate doa with programmable metasurface. *IEEE Internet of Things Journal*, 8(12):10187–10197, 2021.

[16] Jia Wei Wang, Zi Ai Huang, Qiang Xiao, Wei Han Li, Bai Yang Li, Xiang Wan, and Tie Jun Cui. High-precision direction-of-arrival estimations using digital programmable metasurface. *Advanced Intelligent Systems*, 4(4):2100164, 2022.

[17] Jia Wei Wang, Zi Ai Huang, Xiang Wan, Wen Hao Wang, Bai Yang Li, Jie Li, Qiang Xiao, Wei Han Li, and Tie Jun Cui. Polarization and direction-of-arrival estimations based on orthogonally polarized digital programmable metasurfaces. *Journal of Physics D: Applied Physics*, 56(46):465001, aug 2023.

[18] The Viet Hoang, Vincent Fusco, Muhammad Ali Babar Abbasi, and Okan Yurduseven. Single-pixel polarimetric direction of arrival estimation using programmable coding metasurface aperture. *Scientific Reports*, 11(1), 12 2021.

[19] E.J. Candes, J. Romberg, and T. Tao. Robust uncertainty principles: exact signal reconstruction from highly incomplete frequency information. *IEEE Transactions on Information Theory*, 52(2):489–509, 2006.

[20] Richard G. Baraniuk. Compressive sensing [lecture notes]. *IEEE Signal Processing Magazine*, 24(4):118–121, 2007.

[21] Victor J. Barranca, Gregor Kovačič, Douglas Zhou, and David Cai. Improved compressive sensing of natural scenes using localized random sampling. *Scientific Reports*, 6(1), 8 2016.

[22] Xiao Qing Chen, Lei Zhang, Shuo Liu, and Tie Jun Cui. Artificial neural network for direction-of-arrival estimation and secure wireless communications via space-time-coding digital metasurfaces. *Advanced Optical Materials*, 10(23):2201900, 2022.

[23] Xiaoyi Wang and Christophe Caloz. Direction-of-arrival (doa) estimation based on spacetime-modulated metasurface. In *2019 IEEE International Symposium on Antennas and Propagation and USNC-URSI Radio Science Meeting*, pages 1613–1614, 2019.

[24] Xinyu Fang, Mengmeng Li, Juzheng Han, Davide Ramaccia, Alessandro Toscano, Filiberto Bilotti, and Dazhi Ding. Accurate direction–of–arrival estimation method based on space–time modulated metasurface. *IEEE Transactions on Antennas and Propagation*, 70(11):10951–10964, 2022.

[25] Jun Yan Dai, Wankai Tang, Manting Wang, Ming Zheng Chen, Qiang Cheng, Shi Jin, Tie Jun Cui, and Chi Hou Chan. Simultaneous in situ direction finding and field manipulation based on space-time-coding digital metasurface. *IEEE Transactions on Antennas and Propagation*, 70(6):4774–4783, 2022.

[26] Dexiao Xia, Xin Wang, Jiaqi Han, Hao Xue, Gongxu Liu, Yan Shi, Long Li, and Tie Jun Cui. Accurate 2-d doa estimation based on active metasurface with nonuniformly periodic time modulation. *IEEE Transactions on Microwave Theory and Techniques*, 71(8):3424–3435, 2023.

[27] Qun Yan Zhou, Jun Wei Wu, Si Ran Wang, Zu Qi Fang, Li Jie Wu, Jun Chen Ke, Jun Yan Dai, Tie Jun Cui, and Qiang Cheng. Two-dimensional direction-of-arrival estimation based on time-domain-coding digital metasurface. *Applied Physics Letters*, 121(18):181702, 11 2022.

[28] Hou-Tong Chen, Willie J. Padilla, Michael J. Cich, Abul K. Azad, Richard D. Averitt, and Antoinette J. Taylor. A metamaterial solid-state terahertz phase modulator. *Nature Photonics*, 3(3):148–151, 2 2009.

[29] Hou-Tong Chen, Willie J. Padilla, Joshua M. O. Zide, Arthur C. Gossard, Antoinette J. Taylor, and Richard D. Averitt. Active terahertz metamaterial devices. *Nature*, 444(7119):597–600, 11 2006.

[30] N. Karl, K. Reichel, H.-T. Chen, A. J. Taylor, I. Brener, A. Benz, J. L. Reno, R. Mendis, and D. M. Mittleman. An electrically driven terahertz metamaterial diffractive modulator with more than 20 db of dynamic range. *Applied Physics Letters*, 104(9), 3 2014.